

Found: C, 47.11; H, 5.69; N, 5.31. **1-(*n*-Butyl)pyridinium Iodide (1f)**. Anal. Calcd for  $C_9H_{14}IN \cdot 0.5H_2O$ : C, 39.72; H, 5.56; N, 5.17. Found: C, 40.04; H, 5.58; N, 5.17. **1-(2-Methylpropyl)pyridinium Bromide (1h)**. Anal. Calcd for  $C_9H_{14}BrN \cdot H_2O$ : C, 46.17; H, 6.89; N, 5.98. Found: C, 45.90; H, 7.01; N, 5.70. **1-(1-Methylpropyl)pyridinium Bromide (1i)**. Anal. Calcd for  $C_9H_{14}BrN \cdot H_2O$ : C, 46.17; H, 6.89; N, 5.98. Found: C, 46.25; H, 6.52; N, 6.10. **1-(Cyclopentyl)pyridinium Perchlorate (1l)**. Anal. Calcd for  $C_{10}H_{14}ClNO_4 \cdot H_2O$ : C, 42.64; H, 5.73; N, 4.97. Found: C, 42.66; H, 5.63; N, 4.77. **1-(Cyclopropylmethyl)pyridinium Perchlorate**

(1m). Anal. Calcd for  $C_9H_{12}ClNO_4$ : C, 46.27; H, 5.18; N, 5.99. Found: C, 46.26; H, 5.16; N, 5.97. **1-(Cyclobutylmethyl)pyridinium Perchlorate (1n)**. Anal. Calcd for  $C_{12}H_{18}ClNO_4$ : C, 52.27; H, 6.58; N, 5.08. Found: C, 51.87; H, 6.50; N, 5.14.

**Acknowledgment.** We thank Professor M. Szafran for advice and help with the MO calculations. J.R.E. and C.H.W. acknowledge the Office of Naval Research for partial support of this work.

## Target Gas Excitation in Collision-Induced Dissociation: A Reinvestigation of Energy Loss in Collisional Activation of Molecular Ions of Chlorophyll-*a*<sup>†</sup>

A. J. Alexander,<sup>‡</sup> P. Thibault,<sup>§</sup> and R. K. Boyd\*

Contribution from the Atlantic Research Laboratory, National Research Council of Canada, 1411 Oxford Street, Halifax, Nova Scotia, Canada B3H 3Z1. Received March 13, 1989. Revised Manuscript Received November 27, 1989

**Abstract:** Losses of translational energy accompanying collisional activation (CA) of large organic ions at keV energies have been found to be unexpectedly large, as exemplified by work of Bricker and Russell (*J. Am. Chem. Soc.* **1986**, *108*, 6174) on molecular ions of chlorophyll-*a*. These energy shifts are of practical importance for tandem mass spectrometry applied to biochemistry and are also of theoretical interest with respect to the very large kinetic shifts thus implied for the dissociation. The original work attributed the chlorophyll-*a* shifts to ionization of collision target molecules as a mandatory accompaniment to CA, with negligible contributions from kinetic shift to the observed inelasticity. The present work has exploited improved experimental techniques to demonstrate that those trends observed by Bricker and Russell, which led to their target ionization hypothesis, were experimental artifacts and that target mass rather than ionization energy is the dominant parameter in determining the energy shift. Angular dependences of these energy shifts have been determined and shown to be consistent with predictions based on theoretical calculations of scattering effects based upon the limiting "elastic model" for inelastic collisions. These calculations required only one arbitrarily adjustable parameter (the magnitude of the average energy deposition leading to dissociation) and can account semiquantitatively for energy shifts as well as qualitatively for variations in peak shapes. The limitations of the present approach have also been assessed.

Tandem mass spectrometry has become a widely accepted approach to structural analysis,<sup>1</sup> more recently in the context of larger molecules of biochemical interest. The dissociation of precursor ions, which have been subjected to collisional activation (CA) via collisions at keV energies with a target gas, is often characterized<sup>2</sup> by a substantial loss of translational energy of the precursor ( $E_p$ ). Of course the conversion of translational to internal energy provides the basis for the CA method, but the surprisingly large magnitudes observed for some of these energy-loss shifts, particularly for larger ions, have raised interest in the phenomenon for both practical and theoretical reasons. Thus the widely used technique of mass-analyzed ion kinetic energy spectrometry (MIKES<sup>3</sup>) is subject to the direct effect of such shifts, which greatly reduce confidence in the fragment masses assigned to the observed peaks. If a double-focussing combination of electric plus magnetic sectors is used as the fragment ion analyzer, the energy focussing properties ensure that mass assignments are not affected by energy-loss shifts. However a significant loss in sensitivity can result since the linked-scan relationship for such analyzers is usually calculated on the assumption that such shifts are negligible; by electrically floating the collision region above ground, these practical problems can be alleviated to some extent.<sup>4</sup> The more theoretical interest in these apparently anomalously large energy losses concerns the large

kinetic shifts thus implied for the subsequent dissociation of the collisionally activated ions, on the appropriate time scale (few  $\mu$ s).

A widely quoted example of this phenomenon was reported by Bricker and Russell,<sup>5</sup> who studied the collision-induced dissociation (CID) of ions produced by fast atom bombardment (FAB) ionization of chlorophyll-*a*. The major fragmentation reaction,  $m/z$  893.5  $\rightarrow$   $m/z$  614.2, was studied<sup>5</sup> with different inert gases as collision partners by using the MIKES technique. By assuming that the MIKES peak corresponded to fragment ions of  $m/z$  614 (with no unresolved ions of  $m/z$  within a few Da of this value), an assumption later verified,<sup>6</sup> it was possible<sup>5</sup> to predict the position of the peak on the translational energy scale. The experimentally observed energy shifts  $\Delta E_F$ , thus measured for the fragment ions, were converted to the corresponding shifts for the precursors via the simple relation

$$\Delta E_p = \Delta E_F (m_p/m_F) \quad (1)$$

where  $m_p$  and  $m_F$  are the masses of precursor and fragment ions, respectively. The values of  $\Delta E_p$  thus obtained<sup>5</sup> were remarkably

(1) *Tandem Mass Spectrometry*; McLafferty, F. W., Ed.; Wiley-Interscience: New York, 1983.

(2) Neumann, G. M.; Derrick, P. J. *Org. Mass Spectrom.* **1984**, *19*, 165.

(3) Cooks, R. G.; Beynon, J. H.; Caprioli, R. M.; Lester, G. R.; *Metastable Ions*; Elsevier: Amsterdam, 1973.

(4) Boyd, R. K. *Int. J. Mass Spectrom. Ion Proc.* **1987**, *76*, 319.

(5) Bricker, D. L.; Russell, D. H. *J. Am. Chem. Soc.* **1986**, *108*, 6174.

(6) Guevremont, R.; Boyd, R. K. *Int. J. Mass Spectrom. Ion Proc.* **1988**, *84*, 47.

<sup>†</sup> NRCC No. 31133.

<sup>‡</sup> Present address: Department of Chemistry, Cornell University, Ithaca, NY 14853.

<sup>§</sup> Seconded from Biotechnology Research Institute, National Research Council of Canada, Montreal, Canada.

close to the ionization energies of the respective target gases (Figure 5, ref 5).

These findings were interpreted as evidence that, in the keV energy regime, CA of the precursor ion and excitation (possibly involving ionization) of the collision gas are "competitive processes". As is clear from the brief summary of the experimental measurements, given above, the available evidence suggests that target excitation is a necessary *accompaniment* to CID of the precursor. If correct, this conclusion has far-reaching implications for both the practical and theoretical aspects of the energy-loss phenomenon.

The present work arose from a realization that the experimental facilities available to the original investigators<sup>5</sup> were not ideal and that uncertainties are thus introduced into the appropriate interpretation of these data. The most important shortcoming arises from the fact that loss of the phytol side chain from molecular ions of chlorophyll-*a*, to yield fragment ions of  $m/z$  614.2, occurs readily under unimolecular conditions, i.e., without collisions. Therefore each MIKES peak recorded previously<sup>5</sup> represented a composite of fragment ions from unimolecular dissociations (and thus formed with zero loss of translational energy), occurring throughout the length of the field-free region of the instrument, plus ions formed by CID (and thus with significant energy losses). The intrinsic widths of the MIKES peaks, reflecting the translational energies released in the dissociations,<sup>3</sup> are such that it was impossible to resolve unimolecular from CID components of the composite peak. The values of  $\Delta E_F$  measured in this way depend<sup>7</sup> upon the relative lengths of the field-free region and of the collision cell, on the efficiency of the differential pumping between them, on the relative ion optical collection efficiencies from the two regions, and on the degree of collisional attenuation of the precursor intensity.

If provision is made to electrically float the collision cell, fragment ions formed within the cell can readily be distinguished from those formed in the field-free region; the former should be dominated by products of CID reactions, and the corresponding values of  $\Delta E_F$  should then be independent of collision gas pressure over a wide range. This provides a useful practical test of claims that measured  $\Delta E_F$  values are essentially free of interferences from unimolecular dissociation<sup>7</sup> and is the approach adopted here.

Other disadvantages of the apparatus available to the original investigators<sup>5</sup> included a restriction to analogue recording of single MIKES scans; significant improvements in signal/noise ratio, and thus in precision of estimation of  $\Delta E_F$  values, can be obtained by using multiple scan accumulation of digitized spectra. Finally, use of a wider range of collision gases should permit a more stringent test of the proposal that excitation of the target gas is a necessary condition for CID to occur. A preliminary account of part of this work has been presented previously.<sup>8</sup>

### Experimental Section

The tandem hybrid mass spectrometer used in the present work was a VG Analytical ZAB-EQ instrument; this has a higher mass range magnet and associated extended ion optics but is otherwise very similar to the ZAB-Q instrument described in detail previously.<sup>9</sup> In particular, facilities for beam collimation, and for studies of angular effects in the  $z$ -direction (nonfocussing, slit-height direction), are provided. A VG Analytical 11-250J data system was used for instrument control and data acquisition.

Chlorophyll-*a*, purchased from Sigma Chemical Corporation, was dissolved in chloroform to a concentration of approximately  $3 \mu\text{g}/\mu\text{L}$ . About  $3 \mu\text{L}$  of this solution was mixed with  $2 \mu\text{L}$  of 3-nitrobenzyl alcohol on the gold FAB probe tip. Samples were subjected to bombardment by an 8 keV xenon atom beam generated by an IonTech saddle-field gun. Ions thus formed at a source potential of 8 kV were mass-selected by the magnetic sector field (B), subjected to high-energy collisions in the gas cell located within the region between B and the electric sector field (E),

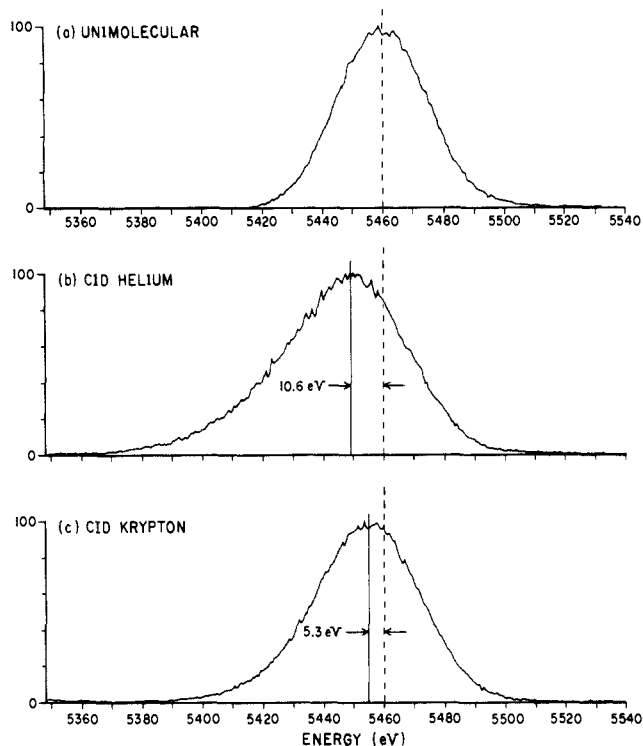


**Figure 1.** Partial MIKE spectra (fragment ion mass region  $m/z$  602–623) of  $M^{++}$  ions of chlorophyll-*a* ( $m/z$  892.5, FAB ionization). Initial translational energy ( $eV_0$ ) of precursor ion 7936.0 eV; collision cell at ground potential. (a) No collision gas; indicated pressure on ion gauge  $8 \times 10^{-9}$  mbar. (b) Helium collision gas admitted to cell until precursor beam intensity attenuated by 50%. (c) Krypton collision gas admitted to cell until precursor beam intensity attenuated by 50%.

and MIKE spectra<sup>3</sup> obtained by scanning E. The energy width of the precursor ion beam, measured with no collision gas, was always less than 5 eV measured as full peak width at half-height. In experiments where the collision cell was electrically floated the cell potential was  $-700$  V from ground, unless otherwise specified. The collision gases were Research Grade from Matheson Gas Products; the pressure of collision gas was adjusted to give approximately 50% attenuation of the precursor beam intensity, except where otherwise noted. Each spectrum represents the accumulation of 16 to 25 scans, corresponding to accumulation times of 5–10 min. The long-term reproducibility (week-to-week) of  $\Delta E_F$  values obtained in this way was  $\pm 1$  eV for the heavier collision gases, and  $\pm 2$  eV for helium, hydrogen, deuterium, and neon; the reproducibility for experiments conducted on the same day was about twice as good.

In angle-resolved experiments the observation angle was defined via a 1 mm high  $z$ -aperture, located between the slit at the point of double-focus and the detector, and which could be moved by up to 5 mm on either side of the main optical axis ( $x$ -axis). The ion beam could be collimated in the  $z$ -direction (slit height direction) by using variable  $z$ -restrictors located between source and magnet (first field-free region) and at the point of intermediate focus (second field-free region); collimation in the  $y$ -direction could be achieved by using the variable  $\alpha$ -restrictor in the first field-free region and an optical slit located 10 cm prior to the slit at the point of intermediate focus (and thus prior to the collision cell). Due to limited available intensity of the precursor ion beam, the degree of collimation applied in practice was appreciably less than the best theoretically achievable (see below).

### Results and Discussion

**(a) Experiments with Collision Cell at Ground Potential.** The region of the MIKE spectrum of the molecular ion of chlorophyll-*a* ( $m/z$  892.5), corresponding to the fragment ion of  $m/z$  614.2 formed with the collision cell at ground potential, is shown in Figure 1 for conditions of no collision gas (Figure 1a, indicated pressure on ion gauge located near the collision cell  $<10^{-8}$  mbar) and also for helium and krypton as collision gases (Figure 1 (parts b and c, respectively)). Corresponding spectra were obtained for all the noble gases. With gas in the grounded collision cell not only is the peak maximum displaced to lower energies but also the peak shape is now asymmetric with a low-energy tail which is much more pronounced for target gases of low mass (He, H<sub>2</sub>,

(7) Guevremont, R.; Boyd, R. K. *Rapid Commun. Mass Spectrom.* **1988**, 2, 1.

(8) Alexander, A. J.; Boyd, R. K.; Thibault, P. *Proc., 37th Conf. Amer. Soc. Mass Spectrom.* **1989**, 224.

(9) Harrison, A. G.; Mercer, R. S.; Reijner, E. J.; Young, A. B.; Boyd, R. K.; March, R. E.; Porter, C. J. *Int. J. Mass Spectrom. Ion Proc.* **1986**, 74, 13.

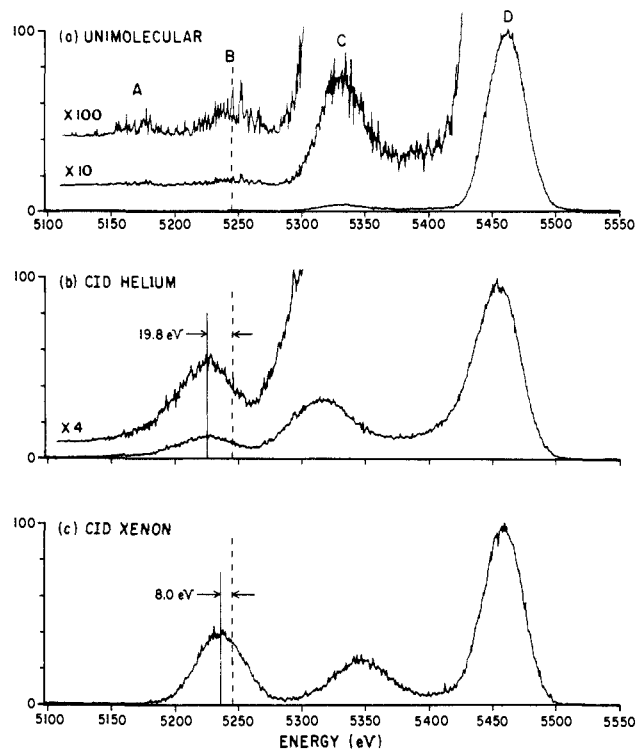


**Figure 2.** Partial MIKE spectra of  $M^{++}$  ions of chlorophyll-*a* ( $m/z$  892.5, FAB ionization) in the region of fragment ions of  $m/z$  614.2. Source accelerating potential  $V_a = 7936.0$  V; collision cell potential  $-700.0$  V: (a) no collision gas; (b) helium collision gas, 50% attenuation of precursor intensity; and (c) xenon collision gas, 50% attenuation of precursor intensity.

$D_2$ ). By repeating these experiments at different pressures of collision gas, it was shown that the energy shifts of the peak maxima and the degrees of peak-tailing asymmetry both increased with increasing attenuation of the precursor intensity. For example, with helium as target gas  $\Delta E_F$  was found to vary from 6 eV at 15% attenuation to 15 eV at 90% attenuation (spectra not shown); the corresponding peak shapes changed from a slightly asymmetric version of Figure 1a to a more broad and highly asymmetric version of Figure 1b, respectively.

These observations are consistent with the interpretation, summarized above, in terms of a composite peak corresponding to a superposition of CID events covering a range of values of  $\Delta E_F$  from zero (no CA) to some maximum, and with different probabilities. (Any one of these events, in isolation, must give rise to a symmetric MIKE peak provided only that the CA step occurs on a time scale well separated from (much shorter than) the subsequent dissociation; this is a simple consequence<sup>3</sup> of the isotropic distribution of fragments in a reference frame fixed relative to the center of mass of the fragmenting species.) Thus, even if the contributions from the unimolecular events can be reduced to insignificant levels, the resulting value of  $\Delta E_F$  is only a most probable value representative of an energy deposition distribution.

**(b) Experiments with a Floated Collision Cell.** The condition of reduction to zero of the unimolecular contribution can be closely approximated by using a short (2 cm) collision cell floated at some convenient electrical potential. The MIKE spectra obtained when the collision cell was floated at  $-700$  V are illustrated in Figure 2. The spectrum obtained without collision gas added (Figure 2a) contains four peaks, for convenience labeled A, B, C, and D. Peak A is present in the spectrum obtained with the cell at ground potential (not shown) and does not correspond to a fragment of  $m/z$  614. By using the techniques described previously<sup>6</sup> to exploit the mass filter properties of the final quadrupole analyzer, it was shown that each of peaks B, C, and D does correspond to only fragment ions of  $m/z$  614.2. The position of peak D was invariant to changes in the potential applied to the collision cell and thus corresponds to fragmentations occurring at ground potential in

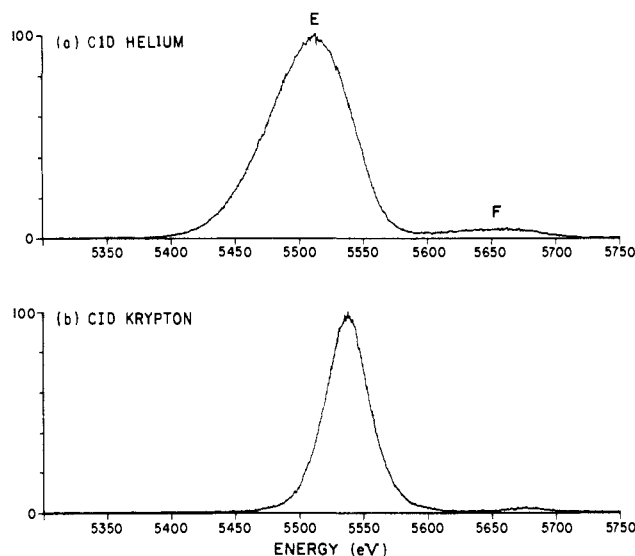


**Figure 3.** Partial MIKE spectra of  $Cs_4I_3^+$  ions, for CID reaction ( $m/z$  912  $\rightarrow$   $m/z$  652). Source accelerating potential 7936.0 V; collision cell potential  $-500.0$  V: (a) helium collision gas and (b) krypton collision gas. In both cases precursor beam intensity was attenuated by 50%.

the field-free region, as in Figure 1a.

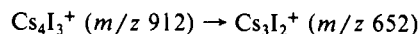
The translational energy of fragments  $F^+$  formed in a cell at potential  $V_c$ , in the absence of any collisional energy loss or kinetic energy release, is given by

$$TE \text{ of } F^+ = eV_a(m_F/m_p) + eV_c(1 - m_F/m_p) \quad (2)$$

where  $V_a$  is the (ion source) accelerating potential. The position of peak B (Figure 2a) varied with  $V_c$  in accord with predictions of eq 2, to within  $\pm 2$  eV, and thus corresponds to unimolecular fragmentations occurring within the floated cell. Thus the displacements of peak B, due to use of various collision gases, are the desired quantities in this work, and these are described below. It is easily shown that eq 1 also applies to values of  $\Delta E_F$  obtained by using nonzero values of  $V_c$ .

However peak C is more intense than peak B, and some effort was devoted to identifying the origins of these ions of  $m/z$  614.2 and intermediate energies. The position of peak C did vary with  $V_c$  but not in accord with eq 2; in fact the tuning of the lenses and deflectors in the second field-free region markedly affected the position of peak C. When collision gas was used in the floated cell, the peak C position varied with the pressure (evaluated in terms of the percent attenuation of the precursor beam) and the nature of the gas. Thus, for a fixed value (50%) of precursor attenuation and at a fixed tuning condition, peak C moved to higher energies (i.e., toward peak D) as the mass of the target gas was increased; for a given gas an increase in pressure also caused a shift in the position of peak C toward that of peak D. In contrast the corresponding positions of peak B (in-cell fragmentations) were invariant (to within experimental precision) to the details of instrument tuning and to collision gas pressure over the range 15–90% attenuation; of course the variations in peak B with nature of the collision gas were the desired objectives of the present work (see below).

We are unable to account in detail for the observed behavior of peak C, summarized above, but it is related to the high efficiency of the fragmentation reaction studied even under unimolecular conditions (Figure 1a); thus no analogous peak C was observed (Figure 3) under the same conditions for the process



for which the unimolecular fragmentation efficiency is much lower. In addition the intermediate energy for peak C indicates that it corresponds to fragmentation reactions occurring at a potential intermediate between  $V_c$  and ground. In fact the collision cell is in electrical contact with components (including the optical slit at the point of intermediate focus) on either side, in order to avoid

large potential differences in locations where the gas pressure may become sufficiently high to sustain a discharge. Thus extended regions of intermediate potential exist; the relative intensity of peak C under unimolecular conditions (Figure 2a) implies that, under typical tuning conditions, fragment ions formed in at least one of these regions must be collected and transmitted with high efficiency by the electric sector analyzer. The variations in position of peak C with pressure and nature of collision gas must then reflect different compromises between gas effusion rates (vary with  $m_T^{-1/2}$ ), and thus gas density distributions outside the cell, and the focussing effects just mentioned. It did not seem appropriate to pursue this question further, since peak B is clearly the feature of interest, and its position on the energy scale is wholly insensitive to these variations. However these observations do serve as a more general warning to these using a floated collision cell in conjunction with the MIKES technique.

The raw data are exemplified by Figure 2 (parts b and c). The values of  $\Delta E_F$  thus derived from the collisionally shifted versions of peak B were converted to  $\Delta E_p$  via eq 1 and are shown in Figure 4; the data represent averages of results obtained on different occasions and with collision gas pressures corresponding to attenuations of the precursor beam intensity covering the range 15–90%. The quoted energy-loss shifts were measured relative to the mean energy of the in-cell fragments (peak B, figure 2a) formed in the absence of collision gas. However, this reference point was itself checked against the position predicted, via eq 2, from the value of  $V_a$  measured on the same scale and found to agree with this prediction to within  $\pm 1$  eV. All of these results are plotted in Figure 4, together with the original data of Bricker and Russell,<sup>5</sup> for comparison.

The differences between the two sets of data, obtained by using a grounded collision cell with noble gas targets, reflect the different experimental parameters including relative lengths of cell and field-free region, details of ion optics, different collisional attenuations of the precursor beam intensity (50% compared with 10–25% previously<sup>5</sup>), etc. Such variation of  $\Delta E_p$  values measured in this way precludes any interpretation in terms of fundamental physical aspects of the collisions. However, note that even here the close similarity of the values observed in the present work, for He and D<sub>2</sub> as collision gases (ionization energies<sup>10</sup> of 24.6 and 15.4 eV, respectively), suggests that the interpretation of  $\Delta E_p$  in terms of ionization of the target gas<sup>5</sup> cannot be generally valid.

The present values of  $\Delta E_p$  extracted from the floated cell experiments are at least independent of gas pressure over a wide range and thus reflect the CA process in some reproducible fashion. These data (Figure 4) show that the experimental values of  $\Delta E_p$  do not correlate with ionization energy<sup>10</sup> of the collision gas, as claimed previously;<sup>5</sup> indeed the molecular mass of the target gas is a much superior correlating parameter, though even here the values for all gases tried except He, H<sub>2</sub>, and D<sub>2</sub> are barely distinguishable from one another despite a target mass variation from that of argon to that of xenon. (Neon and N<sub>2</sub> represent marginally distinguishable cases, Figure 4.) Any self-consistent interpretation of these observations must deal with this striking categorization of targets into very light molecules (H<sub>2</sub>, D<sub>2</sub>, and He) and the rest. This is discussed in section c below.

Variation of the nature of the collision gas also markedly altered the CID peak shape in addition to peak position. The lower mass targets (e.g., helium, Figure 2b), which led to larger values of  $\Delta E_p$ , also gave MIKES peaks which were much more broad and asymmetric than the heavier targets (e.g., xenon, Figure 2c). The asymmetry of peak B in Figure 2b is somewhat obscured by peak C, but the effect is clearly seen for Cs<sub>4</sub>I<sub>3</sub><sup>+</sup> precursors in Figure 3 (peak E) since no feature analogous to peak C is present in that case. These different peak shapes imply that the lighter target gases (He, H<sub>2</sub>, and D<sub>2</sub>) not only require a larger mean value of  $\Delta E_p$  to achieve the CID reaction but also that the distributions are much more broad than for the heavier targets (see discussion in a above). The fact that the peak asymmetry is observed for

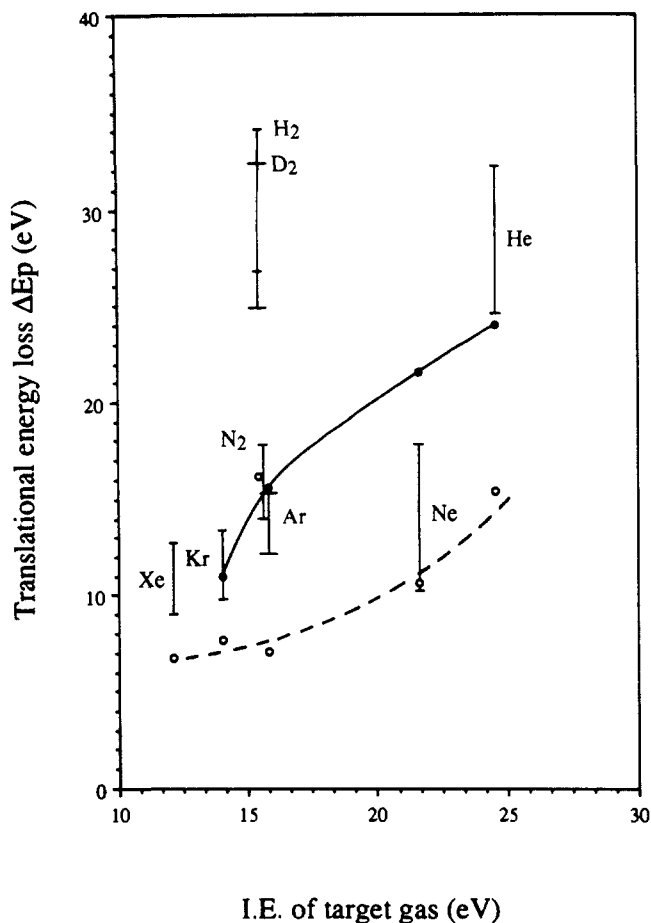


Figure 4. Plot of translational energy loss  $\Delta E_p$  (eV) accompanying CID of the  $M^{++}$  ion of chlorophyll-a, as a function of ionization energy of the target gas. Initial translational energy of precursor was 7936.0 eV. Solid circles represent data obtained with the collision cell at ground potential, estimated from the original work (Figure 5, ref 5); open circles are the comparable data obtained in the present work (month-to-month) reproducibility  $\pm 1$  eV). Data represented by vertical lines were obtained by using a floated collision cell and show ranges of values obtained on several different occasions.

precursors as different as chlorophyll-a and cesium iodide clusters strongly indicates that its origins are unlikely to be chemical in nature. The more fundamental significance of these findings is also discussed in section c below.

(c) **Investigations of Angular Dependence.** Cylindrical electric sector fields, as usually employed in MIKE spectrometry, are dispersive energy analyzers with direction-focussing properties in the same spatial direction (here referred to as the  $y$ -direction, with the main optical axis denoted as the  $x$ -axis). Therefore the MIKES peaks actually observed represent a convolution of the translational energy loss and release, associated with the dissociations, with the ion-optical dispersion and focussing properties of the electric sector. Early attempts<sup>11,12</sup> to deconvolute the ion-optical effects out of the observed peak shapes, to yield the fundamental energy information, were later shown<sup>13,14</sup> to be unreliable; meticulous beam collimation as close as possible to the  $x$ -axis, both before and after the collision cell, is necessary if energy resolution and quantitative energy information are to be obtained. Examples of energy resolution, achievable by eliminating interferences from angular scattering via such collimation, have been

(11) Terwilliger, D. T.; Beynon, J. H.; Cooks, R. G. *Proc. Roy. Soc. London A* 1974, 341, 135.

(12) Terwilliger, D. T.; Elder, J. F.; Beynon, J. H.; Cooks, R. G. *Int. J. Mass Spectrom. Ion Phys.* 1975, 16, 225.

(13) Szulejko, J. E.; Mendez Amaya, A.; Morgan, R. P.; Brenton, A. G.; Beynon, J. H. *Proc. Roy. Soc. London A* 1980, 373, 1.

(14) Mendez Amaya, A.; Brenton, A. G.; Szulejko, J. E.; Beynon, J. H. *Proc. Roy. Soc. London A* 1980, 373, 13.

(10) Rosenstock, H. M.; Draxl, K.; Steiner, B. W.; Herron, J. T. *Energetics of Gaseous Ions. J. Phys. Chem. Ref. Data* 1977, 6, Suppl. 1.

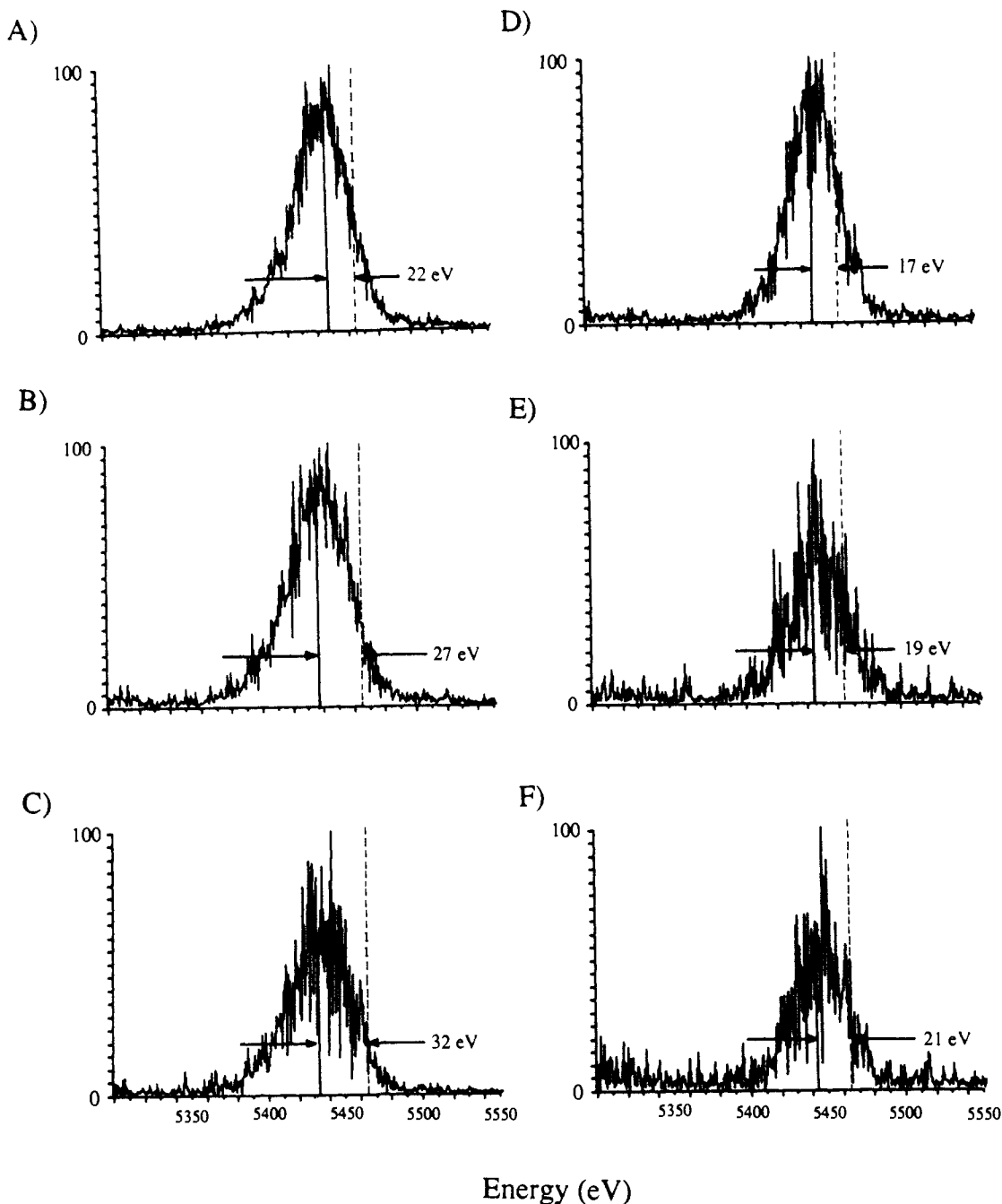


**Figure 5.** MIKES spectra obtained for a collimated beam of  $M^{2+}$  ions from chlorophyll-*a*, for different displacements of a 1 mm high *z*-aperture from the central beam position (main optical axis). Initial translational energy is 7936 eV; collision cell at ground potential: (A, B, C) helium collision gas and (D, E, F) krypton collision gas. *z*-Displacements 0, 2.5, and 4.0 mm for (A, D), (B, E), and (C, F), respectively. Dashed lines indicate predicted positions for zero energy loss, confirmed experimentally (no collision gas) for displacements up to 2 mm.

published.<sup>15</sup> In addition angular variations may be studied by exploiting the lack of focussing action of an ideal cylindrical sector field in the nondispersing direction (*z*-direction);<sup>16</sup> examples of applications include studies<sup>16</sup> of nondissociative electronic transitions (including charge stripping) and variations of translational energy release with observation angle for CID reactions.<sup>17</sup>

The present investigation of angular effects is analogous to this last work,<sup>17</sup> with the distinction that the principal interest now lies in the translational energy loss (peak position) rather than in the peak width. Ideally a floated collision cell should have been used, together with strict collimation in both the *y*- and *z*-direc-

tions, to specify the instrumental observation angle as tightly as possible. Unfortunately considerations of available beam intensity forced compromises to be made. The results reported here were obtained by using the cell at ground potential, with a degree of collimation which was more stringent in the *z*-direction since it was shown previously<sup>16b</sup> that it is more important to collimate in the direction in which the angular displacement is to be defined. The movable *z*-aperture<sup>9,16,17</sup> could be moved by up to 5 mm on either side of the *x*-axis, corresponding to a maximum value of the instrumental observation angle of  $0.28^\circ$  for fragment ions originating in the collision cell; floating the latter would have been an ideal procedure in this context, but the available intensity was too low. The effective angular resolution is difficult to estimate in view of the experimental compromises but was probably no better than  $\pm 0.05^\circ$ , as estimated below. In addition the collision gas pressure was much higher in these experiments than that used to obtain Figure 1 (parts b and c), again in order to optimize the

(15) Brenton, A. G.; Proctor, C. J.; Beynon, J. H. *Adv. Mass Spectrom.* **1980**, *8*, 1689.

(16) (a) Boyd, R. K.; Kingston, E. E.; Brenton, A. G.; Beynon, J. H. *Proc. Roy. Soc. London A* **1984**, *392*, 59. (b) *Ibid.* 89.

(17) (a) Singh, S.; Boyd, R. K.; Harris, F. M.; Beynon, J. H. *Int. J. Mass Spectrom. Ion Proc.* **1985**, *66*, 131. (b) *Ibid.* 151.

signal/noise ratio; this accounts for the generally higher level of energy shifts observed.

Despite these experimental limitations it was possible to observe significant effects in the angle-resolved MIKE spectra, illustrated in Figure 5. The values of  $\Delta E_p$  for krypton as collision gas were almost invariant to changes in observation angle, to within experimental uncertainty, while those for helium showed a significant increase as the angle was increased (Figure 6). The position of the maximum of the peak due to unimolecular fragmentations was invariant to  $z$ -displacement over the range for which it was observable (up to 2 mm). The degree of asymmetry of the peaks obtained by using helium as collision gas (Figure 5a), while difficult to quantify, was noticeably *less* than that evident in Figure 1a; these latter results represent integrations over the entire range of the  $z$ -position variable in Figure 5, (though at lower values of precursor attenuation). Of course, each of the spectra shown in Figure 5 represents an integration over a limited range of the  $z$ -displacement, corresponding to the limited degree of beam collimation which could be imposed. These observations are discussed further below.

Before attempting any interpretation of these trends, however, it is necessary to consider the effects of translational energy release upon the distribution of fragment intensity in the  $z$ -direction at the focal plane of the electric sector; this question has been considered previously,<sup>16a,18,19</sup> in the context of its interference with angle-resolved MIKES experiments. Here a simplified approach<sup>16a</sup> is applied to establish limits for this effect in the present case. For fragment ions ejected from the center-of-mass in any direction (e.g., the  $z$ -direction) orthogonal to the original velocity vector of the precursor (here assumed to be along the  $x$ -axis despite the imperfect collimation employed), the transverse velocity  $\mu_F$  is simply related to the translational energy release  $W$  via

$$\mu_F = [2W \cdot (m_p - m_F) / (m_p \cdot m_F)]^{1/2} \quad (3)$$

so that  $\phi_F$ , the angle to the  $x$ -axis of the trajectory of a fragment ejected along the  $z$ -axis, due to the effect of  $W$  only, is

$$\phi_F = \tan^{-1} (\mu_F / v_F) = \tan^{-1} \{ [(W/eV_a) \cdot (m_p - m_F) / m_F]^{1/2} \} \quad (4)$$

where  $v_F$  is the velocity component along the  $x$ -axis, given to a good approximation<sup>3</sup> by that of the precursor. For the unimolecular fragmentation,  $W$  evaluated from peak width at 20% of peak height (Figure 1a) is 0.10 eV; substitution in eq 4 now gives a predicted value for  $\phi_F$  of 0.14°. Experimentally (data not shown) the intensity of the fragments formed by unimolecular reactions vanished into the noise background at a  $z$ -displacement of about 2.0 mm; this condition was arbitrarily assumed to correspond to 20% of peak height in Figure 1a. This limiting displacement permits an estimate for  $\phi_F$  of 0.12°, if it is assumed that the collection efficiency for fragment ions is dominated by that for fragments originating near the point of intermediate focus (object slit for the electric sector and close to the collision cell). The agreement between predicted and observed values is gratifying, given the approximations made; the approximate model used should be most accurate for estimates of such observational limits rather than for detailed distributions.<sup>18,19</sup>

The MIKES peaks obtained under CID conditions could be recorded with adequate signal/noise ratios for  $z$ -displacements up to 4.5 mm (Figure 6), corresponding to  $\phi_F = 0.26^\circ$ . It therefore appears that the data plotted in Figure 6 do reflect the collisional process although the intensity distribution arising directly from the translational energy release limits the effective angular resolution to about 0.05°, corresponding to the  $z$ -displacement at which the unimolecular intensity drops to 50% of its on-axis value. The very broad MIKES peak obtained (Figure 1b), via helium CID with no  $z$ -discrimination, is asymmetric. This effect cannot be due primarily to an increase in  $W$  (which would give rise to *symmetric* broadening) but must arise from superposition of peaks

(18) Todd, P. J.; Warmack, P. J.; McBay, E. J. *Int. J. Mass Spectrom. Ion Phys.* **1983**, *50*, 299.

(19) Waddell, D. S.; Boyd, R. K.; Brenton, A. G.; Beynon, J. H. *Int. J. Mass Spectrom. Ion Proc.* **1986**, *68*, 71.

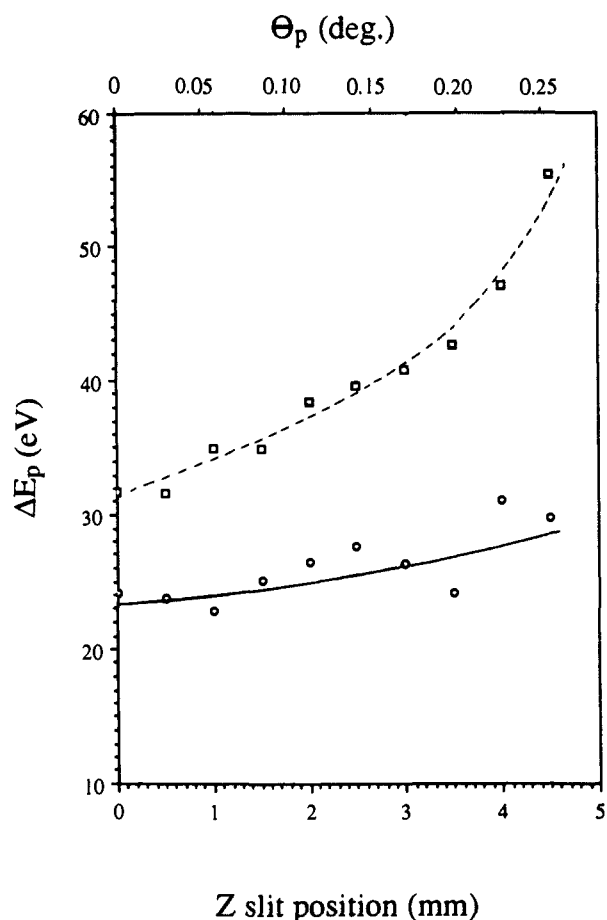


Figure 6. Variation of  $\Delta E_p$  with observation angle, defined via  $z$ -displacement of a movable 1 mm-high  $z$ -aperture, for molecular ions of chlorophyll-*a* undergoing the CID reaction ( $m/z$  892.5  $\rightarrow$   $m/z$  614.2). Uncertainty in  $\Delta E_p$  was  $\pm 3$  eV, less at smaller displacements. The transformation of  $z$ -displacement to  $\theta_p$  is subject to uncertainty (see text) of at least  $\pm 0.05^\circ$ . Squares and circles represent data obtained by using He and Kr, respectively, as collision gas.

corresponding to a range of values of  $\Delta E_p$ . When the range of  $\Delta E_p$  values thus superimposed was limited via beam collimation and angular selection (Figure 5), the degree of asymmetry was indeed reduced as expected.

Having established that the trends apparent in Figure 6 represent a real difference between the CA behavior of one of the very light collision gases and that of one of the heavier targets, it remains to attempt an interpretation of this difference. To this end, theoretical results given previously<sup>16a</sup> have been applied to conditions appropriate to the present experimental work. For inelastic collisions of a projectile ion  $P^+$  with a thermal target gas atom  $T$ , considered in the so-called "elastic" limit where the collision partners are assumed to be structureless so that momentum exchange involves the entire mass of each, the following relationship is a simple consequence<sup>16a</sup> of conservation of energy and of linear momentum (both axial and transverse)

$$Q/E_p^\circ = [1 - (m_p/m_T)] - [1 + (m_p/m_T)] \cdot [1 - (\Delta E_p/E_p^\circ)] + 2(m_p/m_T) \cdot \cos \theta_p \cdot [1 - (\Delta E_p/E_p^\circ)]^{1/2} \quad (5)$$

where  $Q$  is the total inelasticity (internal energy gain of both  $P^+$  and  $T$ ),  $E_p^\circ$  is the initial translational energy of  $P^+$  in the laboratory-fixed reference frame, and  $\theta_p$  is the scattering angle for  $P^+$  again in the laboratory frame; it was also assumed that the precollision translational energy of  $T$  is negligible. Note that, in the derivation of eq 5, no account was taken of the  $T$ - $P^+$  interaction potential and the initial conditions for the collision (impact parameter, etc.), so that no information is available concerning relative cross sections for the competing processes considered below. In addition eq 5 clearly refers to single collisions, a condition not met in the experiments.

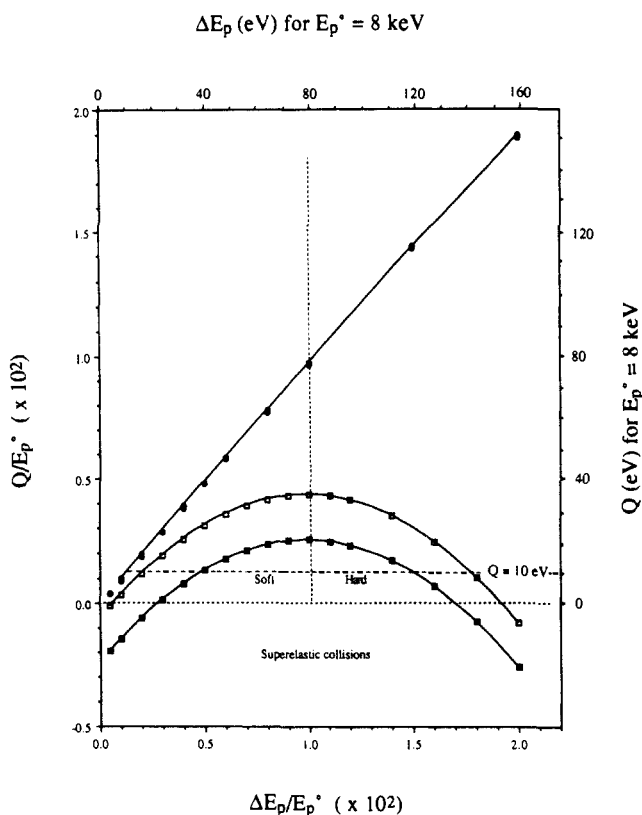


**Figure 7.** Theoretical predictions of inelasticity  $Q$  accompanying collisional activation of projectile ions (mass  $m_p$ ) via collisions with thermal targets  $T$  (assumed initially stationary), for specified values of projectile scattering angle  $\theta_p$  ( $0.1$  and  $0.2^\circ$  for open and closed symbols, respectively), as a function of the total loss of translational energy  $\Delta E_p$ . Squares and circles refer to values of  $(m_p/m_T) = 200$  (simulating chlorophyll-*a* on helium) and  $10$  (chlorophyll-*a* on krypton), respectively. Absolute energy scales refer to an incident projectile energy  $E_p^*$  of  $8$  keV. All quantities are defined relative to a laboratory-fixed reference frame. Calculations were based on the "elastic limit" model (see text, eq 5).

Evaluation of eq 5 has been carried out for  $(m_p/m_T)$  ratios of  $10$  and  $200$  (corresponding approximately to  $M^{++}$  ions of chlorophyll-*a* in collision with Kr and He, respectively) and for scattering angles  $\theta_p$  of  $0.2$  and  $0.1^\circ$  (corresponding approximately to the maximum and median values, respectively, imposed by the  $z$ -dimensions of the final slit (see above)). The results thus obtained are shown in Figure 7 and are qualitatively similar to those obtained previously<sup>16a</sup> for different values of the parameters. The deviation of  $Q$  from the value of  $\Delta E_p$  represents  $E_T$ , the post-collision translational energy of the target  $T$ . In general,  $E_T$  must be larger for a light than for a heavy target, in order that the post-collision transverse momentum of  $T$  may balance that of  $P^+$ . Other general comments on the form of these curves may be found in the previous work;<sup>16a</sup> in particular the cross sections for the "hard" collisions (Figure 7) are much smaller than those for the "soft" collisions corresponding to the same value of  $Q$ . In the present context the important aspects are the qualitative difference between the curves for light and heavy targets and the marked dependence on  $\theta_p$  of the curves for the light target. (The angles  $\theta_F$  predicted for observation of the *fragment* ions are the same as  $\theta_p$ , except for the symmetrical broadening due to effects of  $W$ , eq 4.)

Suppose that, for those  $M^{++}$  ions of chlorophyll-*a* which do not possess sufficient internal energy to fragment unimolecularly, an additional energy increment  $Q$  of  $10$  eV is required in order that the fragmentation rate constant can match the experimental time scale; the reasons for choosing this particular speculative value will become apparent below. Calculations based on eq 5 (see also Figure 7) then predict that, for a heavy target such as krypton ( $m_p/m_T = 10$ , approximately), this value of  $Q$  should be achieved with values of  $\Delta E_p$  ranging from  $10.1$  eV (for  $\theta_p$  close to zero) to  $11$  eV (for  $\theta_p$  of  $0.25^\circ$ , close to the instrumental maximum for

scattering in the  $z$ -direction). For those experiments in which no  $z$ -collimation was applied (Figure 2c) and for which the observed MIKES peak thus corresponds to an appropriate integration over  $\theta_p$  ( $z$ -height), this result implies that  $\Delta E_p$  for a heavy target should fall in the range  $10$ – $11$  eV, as observed in Figure 4. This limiting value of about  $11$  eV for heavy targets led to the above estimate of  $10$  eV for  $Q$ ; this is the only arbitrarily fixed parameter in the present treatment. Moreover the corresponding peak shapes should not be too different from that for fragmentations observed in absence of collision gas, since the superimposed peaks are displaced from one another by a maximum of  $1$  eV (see above), well within the experimental uncertainty. The precise position of the peak maximum cannot, in principle, be predicted from the present theoretical considerations since no information is available concerning relative cross sections, which control the weighting function for the integration over  $\theta_p$ . Predictions for those experiments in which  $z$ -collimation was applied, to permit some degree of resolution in  $\theta_p$ , are that no significant variation of  $E_p$  with  $\theta_p$  should occur for such heavy targets; this is in accord with experimental observation (Figures 5 and 6). Calculations (not shown) based on eq 5 for  $(m_p/m_T) = 20$ , simulating chlorophyll-*a* in collision with argon, confirm that in the appropriate range the predicted curves are very close to those for  $(m_p/m_T) = 10$  (simulating  $T =$  krypton); this is also in accord with experimental observation (Figure 4) and accounts for the insensitivity of  $\Delta E_p$  values to variations in  $m_T$  for other than the very light targets (section b above).

If the present approach is valid, the value of  $Q$  should be independent of the nature of the target, since it is defined only by the properties of the projectile ions as they enter the collision region and by the dimensions of the apparatus via the experimental time scale. Then for the same estimate of  $10$  eV for  $Q$ , eq 5 (see also Figure 7) predicts that for  $m_p/m_T = 200$  ( $T =$  He in the present case) the corresponding values of  $\Delta E_p$  should vary from about  $10.5$  to  $50$  eV over the appropriate range for  $\theta_p$ . This prediction is in semiquantitative agreement with observation (Figure 6), bearing in mind the limited angular resolution and the superimposed effects of  $W$  (eq 4). In this case ( $T =$  He) the question of the (unknown) relative cross sections, for different values of  $\theta_p$  with this fixed value for  $Q$ , becomes crucial with respect to the integration over  $\theta_p$  to give the predicted peak shape, and thus the position of the peak maximum, in the absence of angular resolution. Nonetheless the observed integrated peak shape (Figure 2b) is generally consistent with the present predictions, bearing in mind the additional smearing effects of translational energy release as discussed above.

The present theoretical considerations can thus account for the qualitative differences (Figure 4) arising from use of very light targets as opposed to heavier collision gases; in this context the standard of mass comparison is the mass of the projectile ion itself since only the ratio  $(m_p/m_T)$  enters the relationships (eq 5). It is appropriate to briefly reiterate the shortcomings of the present approach. The model used for the inelastic collisions (the "elastic" limit) assumes that the entire projectile interacts with the entire target, a concept of dubious validity for helium interacting with chlorophyll-*a*, for example. Nonetheless this does provide one theoretical limit in considerations of scattering associated with collisional activation.<sup>16a</sup> The other limit corresponds to an extreme version of the "binary" or "spectator" model, in which the only portions of each collision partner which interact directly are electrons; in this case, corresponding to longer range collisions and minimal momentum transfer, large inelasticities  $Q$  can be accompanied by negligible scattering.<sup>16a</sup> Less extreme versions of the spectator model visualize rotational–vibrational excitation via internuclear momentum transfer (and thus involving appreciable scattering) between the target gas atom and some portion of the projectile ion;<sup>16a</sup> quantitative evaluation of such models is beset by uncertainties in estimating the split of the total projectile mass between "spectator" and "impact" moieties.

In any real beam-gas experiment the whole range of collision types is sampled, but the observable result (the MIKES peak for dissociation in this case) reflects the relative probabilities for



activation with subsequent dissociation; these relative probabilities will in general vary with the nature of the target, even for a given projectile. The present work considered only the extreme "elastic" limit since this is readily and unambiguously evaluated;<sup>16a</sup> the trends expected for collisions approximating the "binary" limit are qualitatively similar, but with scattering angles which are smaller than those predicted for the "elastic" limit by factors depending on the effective masses of "spectator" and "impact" moieties mentioned above. The foregoing discussion emphasizes that the success of the "elastic limit" approach in the present example may be somewhat fortuitous, presumably reflecting large *dissociative* cross sections for collisions approximating this limit. These cross sections are not available from any such theoretical approach which does not consider interaction potentials, and this also accounts for the lack of predictive capability for peak shapes.

Other ambiguities arise from more phenomenological considerations of limitations on the degree of angular resolution achievable experimentally. These limitations arose from the intrinsic smearing effects of translational energy release<sup>18,19</sup> and also from the available beam intensity which precluded the use of stringent beam collimation as well as of a floated cell. The intensity limitations also led to use of collision gas thicknesses which undoubtedly corresponded to multiple collision conditions; this in turn could have contributed to the differences apparent in Figure 6 via subsequent collisions (both dissociative and non-dissociative) of both the fragment ions and of the precursors. It is difficult to make simple predictions concerning the net effect of multiple collisions, e.g., nondissociative collisions of the fragments can scatter some of these out of the acceptance aperture of the analyzer but can also scatter some which would otherwise have been lost back into the acceptance aperture.

These *caveats* do not invalidate the present interpretation, but it is important to emphasize the limits thus imposed upon it. It should be noted that, apart from the approximations intrinsic to the theoretical model, the only assumption made was the estimated value of  $Q$ . This lack of arbitrariness is a strength of the present approach.

### Conclusions

On a purely empirical level the present experiments have shown that the values of  $\Delta E_p$ , accompanying CID of  $M^{*+}$  ions of chlorophyll-*a*, are *not* related to the ionization energies of the targets but correlate well with target mass. Previous findings<sup>5</sup> of a

correlation with ionization energy have now been shown to be an artifact of the experimental technique used, arising from superposition of unimolecular and CID reactions. When the former contributions were minimized through use of a floated collision cell, values of  $\Delta E_p$  independent of target pressure over a wide range were obtained (Figure 4). The rationale for the previous conclusion,<sup>6</sup> that target excitation (including ionization) *necessarily* accompanies CID, thus no longer exists.

The present interpretation of the observed trends is based upon the assumption that the average inelasticity  $Q$  is deposited entirely on the projectile ion (no excitation of noble gas targets<sup>5</sup>). Values of  $Q$  which can lead to observable CID are controlled only by the characteristics (including internal energy content) of the projectiles as they enter the collision region and by the instrumental dimensions controlling the experimental time scale. On this point of view  $Q$  must be independent of the nature of the target, so that differences between  $\Delta E_p$  values for the various targets must reflect only the details of the collisional scattering. Experimental and theoretical approaches to the angular dependences of  $\Delta E_p$  for different targets have provided an additional dimension of information on this question. A simple theoretical model, based on the "elastic limit" approximation<sup>16a</sup> for inelastic collisions, has been shown to account qualitatively and semiquantitatively for many of these experimental observations of  $M^{*+}$  ions of chlorophyll-*a*; only one adjustable parameter (the value of  $Q$ ) was necessary.

The present work does not, of course, provide the last word on the problem of large energy-loss shifts  $\Delta E_p$ , accompanying CID of large precursor ions at keV energies. Quite apart from the shortcomings summarized above, it is clear that chlorophyll-*a* is a far from ideal system upon which to base fundamental studies of collisional activation and the overall CID process, in view of the intense unimolecular fragmentation spectrum observed (Figure 1a). In this regard current work of Giblin and Gross<sup>20,21</sup> on the energetics of charge-remote fragmentations seems more promising. Nonetheless many of the previously puzzling features of these energy shifts have now been shown to be explicable on the basis of established principles.

(20) Giblin, D. E.; Gross, M. L. *Proc. 36th Ann. Conf. Am. Soc. Mass Spectrom.* **1988**, 83.

(21) Giblin, D. E.; Gross, M. L. *Proc. 37th Ann. Conf. Am. Soc. Mass Spectrom.* **1989**, 238.